Gear ratio selection of an outer-stator magnetically geared machine (repository copy)

Article:

Tlali, P.M., Gerber, S., Wang, R-J. (2014) Gear ratio selection of an outer-stator magnetically geared machine, *Proc. of the Southern African Universities Power Engineering Conference*, (SAUPEC), Durban, South Africa, pp. 242--248, 30-31 January 2014

GEAR RATIO SELECTION OF AN OUTER-STATOR MAGNETICALLY GEARED MACHINE

P.M. Tlali, S. Gerber and R-J. Wang

Department of Electrical and Electronic Engineering
Stellenbosch University, Private Bag X1
Matieland 7602, South Africa
E-mail: 15894215@sun.ac.za

Abstract: The selection of a gear ratio plays a critical role in the design of a magnetically geared electrical machine. It has been shown in literature that the gear ratio selection has a direct impact on the performance of the magnetically geared machine in terms of maximum torque limit, torque quality and core losses. Larger gear ratios are often preferred, which in turn requires greater difference in pole-pair numbers between the rotors of a gear. As a result, high pole-pair number on the low speed rotor is necessary. However, with a high number of pole-pairs, the inter-pole leakage flux tends to be more severe. In this paper, finite element analysis is used to investigate the effects of gear ratios on the performance of an outer-stator type magnetically geared machine. Relevant discussions are given and conclusions are drawn.

Key words: finite element analysis; geared electrical machines; gear ratio; permanent magnet.

1. INTRODUCTION

Geared electrical machines have proven to be more advantageous from the weight, size and output-per-cost perspectives than directly driven machines [1]. Mechanically geared machines are coupled together via shafts in order to achieve the conversion of low-speed / high-torque to low-torque / high-speed or vice-versa. However, the operation of a mechanical gear relies on the physical contact of teeth. Thus mechanical gears have inherent frictional losses and suffer from teeth wearing. Magnetic Gears (MGs) have increasingly received attention in recent years as an alternative technology.

Because of their contact-less operation, inherent overload protection, little or no maintenance, high torque density and efficiency [2, 3], MGs can potentially outperform their mechanical counterparts. Furthermore, they can easily be integrated into permanent magnet (PM) machines to form a more compact design. One notable type of such a magnetically geared machine (MGM), which was first presented in [4], incorporates a coaxial MG inside an outer-stator PM machine, as shown in Fig. 1.

There has been research focused on the influence of different design parameters on the performance of the MGs only. In [5], an investigation was done on the effects of the design parameters on the maximum torque capability of an MG. This study showed that amongst other parameters considered, the gear ratio has the major influence [5]. The same conclusion was proven to hold true for an axial field MG [6], where the optimum pole-pair number was also dependent on the air-gap length between the rotors. An in-depth simulation study on pole-pair combinations of MGs for wind turbine generators was made in [7]. It was concluded that the gear ratio affects both the magnitude

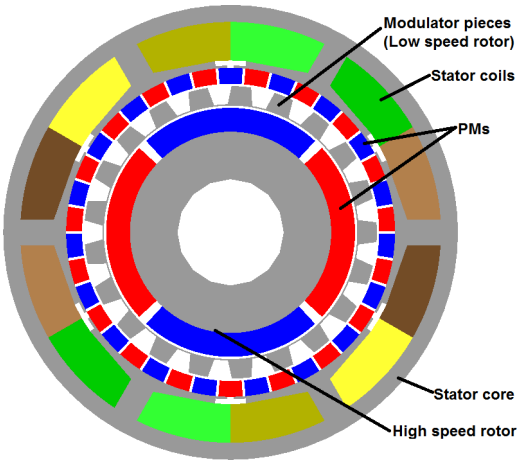

Figure 1: Outer-stator PM magnetically geared machine.

and the quality of torque. Although it was highlighted that there could be a practical limit to the number of pole-pairs used, higher gear ratios were found likely to have less ripples and larger torque capacity [7]. On the other hand, relatively little work has been reported on the impact of the gearing ratio and other design parameters on system torque and efficiency of combined MGMs. Similar to MGs, MGMs exhibit an increase in torque density as the gear ratio increases up to some optimal value [3, 8]. Evans and Zhu [9] conclude that the selection of such a best gear ratio is fundamental to optimal MGM design at a determined volume.

This paper investigates the effects of the gear ratio on the performance of an outer-stator MGM, shown in Fig. 1. Please note that all the designs in this paper are of the same outer radius and stack length. The mechanical layout

of the MGM under study and the relationship between its number of pole-pairs and gear ratios are explained in section 2. In section 3, the simulation setup for optimizing the considered machine and the imposed constraints are described. Section 4 discusses the effects of gear ratios on torque, core losses and some of the machine's component dimensions. Lastly, a conclusion is drawn from the presented results.

2. OUTER-STATOR TYPE MGM

This section briefly describes the main components of the outer-stator MGM and how they interact with each other to accomplish the overall working system. Moreover, the relation between the components' poles and their contribution to the gear ratio are elaborated on.

2.1 *Machine configuration*

The system layout of the MGM investigated in this paper is shown in Fig. 2. It comprises of the high speed PM rotor, low-speed ferromagnetic rotor (modulator) and the outer-stator with non-overlapping windings. Apart from carrying a balanced 3-phase winding, the stator core also supports PMs on its inner surface. These PMs, together with the modulator and high-speed rotor, form the MG part of this machine, while the stator and high speed rotor make up a PM machine.

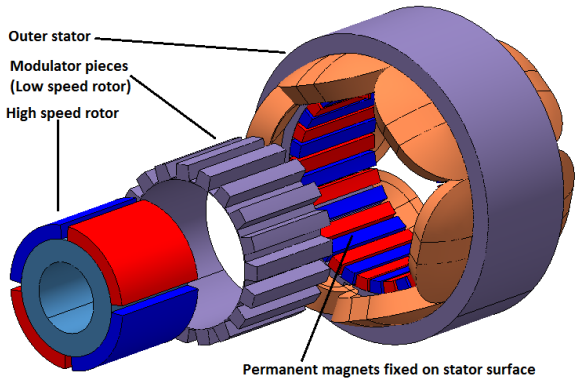

Figure 2: Structure of outer-stator magnetically geared machine.

In this MGM topology, both an MG and a PM machine are housed in a single volume sharing magnetic flux paths and mechanical structure. In this manner, high torque density can be achieved. Compared to the inner-stator type MGM designed in [10], the current topology has one less air-gap and thus a reduced mechanical construction complexity. On the other hand, the comparison study conducted in [11] found that the inner-stator MGM with three air-gaps is still better in both efficiency and torque density.

2.2 *Torque transmission between the components*

There exists two torque components within this type of MGM since it is a combination of two systems in one volume, that is, MG and PM machine. The first component, termed *magnetic torque*, results from the interaction of modulated fields from PMs on the high-speed rotor and field from the fixed PMs on the stator. The second one, called *electromagnetic torque*, is a result of the interaction between the field generated by the stator windings and the fundamental field of the high-speed rotor's PMs. Based on this, the high-speed rotor can be regarded as a coupling medium between the MG and PM machine. The modulator, being the input terminal, carries a large magnitude of magnetic torque. This value then gets scaled down onto the high-speed rotor according to the gear ratio as defined in the next section.

In order to achieve steady state operation, the magnetic torque needs to balance out with the electromagnetic torque experienced by the high speed rotor resulting in a zero net torque on the high speed rotor.

2.3 *Relationship of gear ratio to number of poles*

The basic principle of magnetic gearing operation derived and verified in [3, 12], boils down to two forms of gearing ratio G_r. The main difference between the two modes, illustrated by equations 2 and 3, is determined by whether the ferromagnetic pieces (modulator) or one of the rotors is fixed.

$$q_m = p_h + p_l \tag{1}$$

$$G_r = \frac{q_m}{p_h} \tag{2}$$

$$G_r = \frac{-p_l}{p_h} \tag{3}$$

In the above p_l, p_h and q_m are low-speed rotor pole-pairs, high-speed rotor pole-pairs and ferromagnetic pole-pieces, respectively. The second equation describes the case of MGM studied in this paper since the high number of PMs poles (p_l) are fixed on the inside surface of the stator core. That means the ferromagnetic modulator pieces will now form the low speed input rotor while the inner-most ring forms the high-speed rotor. It can be clearly seen from eqn. (2) that an increase in p_h decreases G_r whereas an increase in p_l increases G_r. Therefore, larger values of G_r can be obtained by maintaining greater difference between p_l and p_h. In synchronous PM machines, the value of p_h is equivalent to stator pole-pairs. Consequently, the selection of this variable has to abide by the stator pole/slot combination rules. This leaves p_l as a variable to be adjusted for different G_r values.

Conventionally, the balanced 3-phase stator can only have a number of slots which are multiples of 3. Likewise, both the stator and the rotor are limited to an even number

of poles. Several applicable stator pole/slot combinations for non-overlapping windings together with their resultant winding factors are listed in [13]. For the current study, the pole/slot combination was selected according to the criteria and procedure presented in [14]. Two stator pole-slot combinations, which can easily be accommodated within a small diameter of the proposed model are 4/6 and 6/9. Therefore, p_h will either be 2 or 3 throughout the entire investigation. The value of p_l is obtained by parameter sweeping through a certain range of numbers excluding those which give an integral G_r.

3. DESIGN OPTIMIZATION ENVIRONMENT

A dedicated design environment for MGMs has been established, which consists of the following three components:

- SEMFEM - In-house developed FEM program.
- MagNet version - 7.1 from Infolytica Corporation.
- VisualDOC version - 7 from VR&D Inc.

Fig. 3 shows the process flow diagram used in the determination of maximum torque capacity at each G_r value. The combination of VisualDOC and SEMFEM is used to optimize the model for maximum torque per mass. This is done within the feasible search range as defined by the fixed dimensions and variable constraints shown in Tables 1 and 2, respectively.

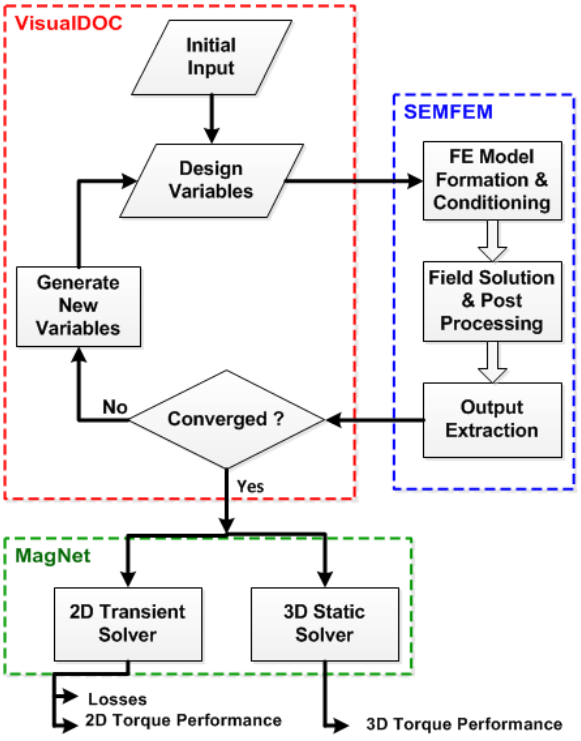

Figure 3: Flow diagram of the design optimization environment.

A gradient based optimization algorithm was used to solve the constrained problem formulated as:

$$\text{Maximize:} \quad F(\mathbf{X}) = \text{Torque } (T_M)/\text{active mass} \tag{4}$$

$$\text{Subject to:} \quad T_E \geq 0.8 \times T_M \tag{5}$$

$$t_{mh}/t_{ms} \leq 1.5 \tag{6}$$

where T_E is the electromagnetic torque, T_M is the magnetic torque on the high speed rotor, t_{mh} and t_{ms} are corresponding thickness of the rotor and stator magnets and, $\mathbf{X}$ represents the variables in Table 2.

As illustrated in Fig. 3, VisualDOC iteratively directs inputs to and retrieves outputs from SEMFEM while also checking their compliance to the defined constraints. The task of SEMFEM is to perform the 2D FEM static simulation for each input set. To enhance the optimization time efficiency, VisualDOC has to be coupled with a fast FEM program. The choice of SEMFEM over MagNet for the above mentioned purpose is justified from Table 3, where the computational time is based on a desktop computer (Intel Core-i7 3.5GHz with 16GB RAM).

Table 1: Fixed geometric variables of the MGM.

Outer diameter of the machine (mm)	140
Stack length of the machine (mm)	50
Air-gaps (mm)	0.7

Table 2: List of design variables.

Description	min	max
Rotor yoke thickness (mm) t_y	8	15
rotor PM thickness (mm) t_{mh}	2.5	8
stator PM thickness (mm) t_{ms}	2.5	8
Rotor/stator PM thickness ratio t_{mh}/t_{ms}	0.667	1.5
PM span to pole-pitch ratio θ_s/θ_p	0.667	0.95
Modulator thickness (mm) t_{md}	6	
Modulator pole pitch ratio θ_{mi}/θ_{md}	0.45	0.7
Stator yoke thickness (mm) t_{sy}	4	-
Stator tooth thickness (mm) t_{st}	6	-
Stator tooth length (mm) l_{st}	10	-
Stator tooth base thickness (mm) t_{sb}	1.5	-
Slot pole to pitch ratio θ_{ss}/θ_{sp}	0.5	0.95
Slot open pitch ratio θ_{so}	0.1	0.5
Slot fill factor	0.3	0.55
Current density (A/mm^2)	1	5
Stator load-factor	0.8	-

Table 3: Computational time of different FEM packages.

Program	Simulation type	CPU Time (sec)
SEMFEM	2D-static	5
MagNet	2D-static	37
MagNet	3D-static	2700
MagNet	2D-transient	2040

Each optimum solution obtained from VisualDOC is then verified with MagNet's 3D static solver. Furthermore, a

2D FE transient simulation is carried out to analyze the transient behavior of that particular design.

The geometrical optimization variables in Table 2 are defined in Figs. 4-6. The modulator, situated between the two PMs sets, will be subjected to large attraction forces even for small imperfections in alignment. Hence, the minimum thickness constraint placed on this component is to ensure its mechanical integrity. The purpose of the thickness ratio between the two sets of PMs is to safeguard them against possible demagnetization, while the minimum PM thickness values take practical manufacturability into account.

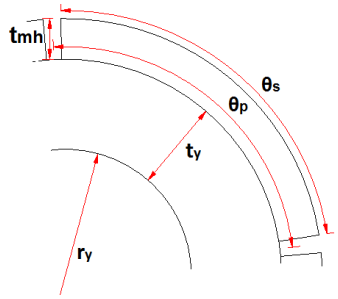

Figure 4: Portion of the MGM's high speed rotor showing design variables.

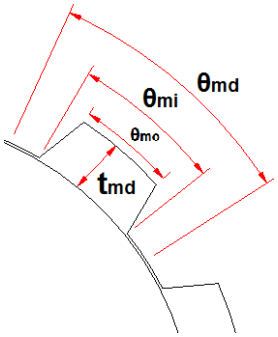

Figure 5: Portion of the MGM's modulator showing design variables.

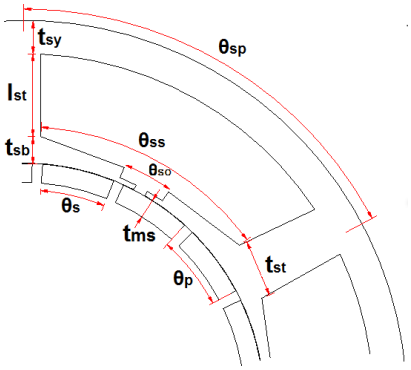

Figure 6: Portion of the MGM's stator showing design variables.

The stator load-factor is defined as the ratio of the stator electromagnetic- to gear's magnetic torques over the high speed rotor. It is constrained to avoid an under designed stator. The current density is limited to 5 A/mm^2 for all the designs since the machine is to be naturally air-cooled.

4. SIMULATION RESULTS

The performance of the MGM in terms of its maximum torque limit and quality, for a range of pole-pair combinations is assessed in this section.

4.1 Maximum torque capacity

The maximum torque capability of the machine as a function of the gear ratio is shown in Fig. 7. The graph includes both 2D and 3D FE simulated results for each of the 4/6 and 6/9 pole-slot combinations. The 3D FE results are around 20% less than those of 2D FE. This difference may be attributed to the 3D end effects which are ignored in the 2D FE solver.

It is important to note that all the graphs in Fig. 7 flatten as the gear ratio increases. The region where a graph's gradient declines significantly contains the preferred pole-pair combinations or the gear ratio values. This is because further increasing the gear ratio results in almost no gain in maximum torque.

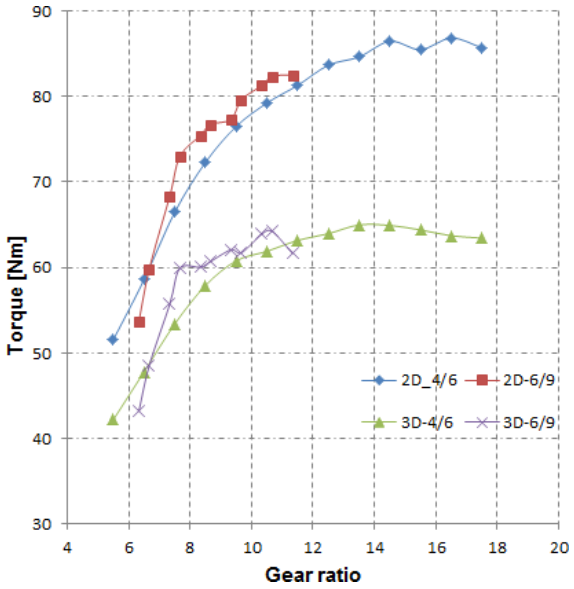

Figure 7: Maximum torque of the outer-stator MGM for different gear ratios.

Figure 8 confirms the stator load factor constraint as defined in section 3. The stator electromagnetic average torque is always around 80% of the maximum magnetic torque on high speed rotor at any instant. In other words, the stator can only be operated continuously up to 80% of the theoretic maximum load of the gear.

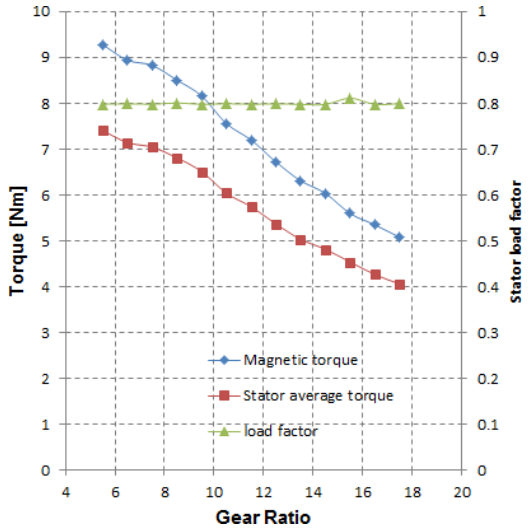

Figure 8: Comparison of electromagnetic and magnetic torques as seen by the high speed rotor showing a complied stator load factor.

4.2 *Iron losses*

The iron losses in this machine includes eddy current and hysteresis components, most of which are occurring in the stator core and modulator. These losses may be calculated by the following equation [15].

$$\begin{aligned} P_{iron} &= P_h + P_e + P_{exc} \\ &= k_h f B_m^{\alpha} + k_e f^2 B_m^2 + k_{exc} f^{1.5} B_m^{1.5} \end{aligned} \tag{7}$$

where B_m is the maximum flux density, f is the flux frequency, k_h, k_e, k_{exc} and α are the material specific loss coefficients which are normally provided by their manufacturers. The operating frequency in this type of MGM whereby the modulator is the mechanical input terminal is expressed in terms of the pole-pieces and input rotation speed as:

$$f = \frac{q_m n_{rpm}}{60} \tag{8}$$

where n_{rpm} is the rotation speed.

For a fixed input speed, the iron losses are a function of pole-pairs and flux density. Fig. 9 shows the plot of average core losses obtained from 2D FE transient analyses as a function of gear ratio.

For each of the two pole-slot combinations (4/6 and 6/9) considered, the iron loss graphs show a steady increase with the gear ratio. This proves that while the increase of G_r could be beneficial to the maximum achievable torque, the escalation of losses could degrade the machine's overall efficiency.

4.3 *Cogging and ripple torque*

The main source of the torque ripple is the cogging torque, which is caused by the interaction between the high speed rotor PMs and stator slots [16]. For MGMs, the cogging torque also depends on the least common multiple (LCM) between the rotors' pole-pair number and stator PMs. It is understood that the higher LCM value results in higher-order lower-amplitude of the cogging and ripple torques. The severity of this torque may be indicated by the so-called *cogging factor* f_c defined by eqn. (9), where p and q are number of pole pairs and slots respectively.

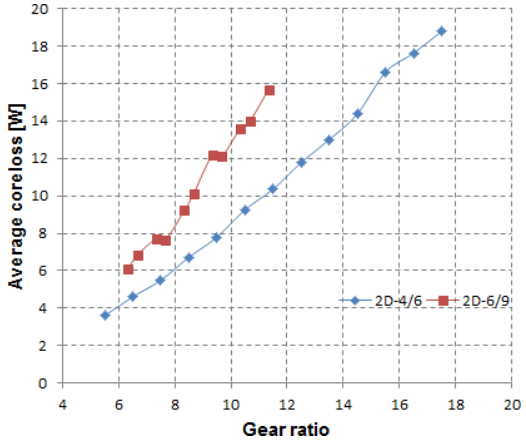

Figure 9: Average iron losses at different gear ratios.

$$f_c = \frac{2pq}{\mathrm{LCM}(p,q)} \tag{9}$$

In [7], the pole-pair combinations with whole, half and 1/3 gear ratios were found to have high cogging torque values. The pole/slot combinations selected for this study limits the gear ratio to either $1/2$ or $1/3$, hence relatively large cogging torque may be expected. Fig. 10 shows the computed cogging torques of the MGM.

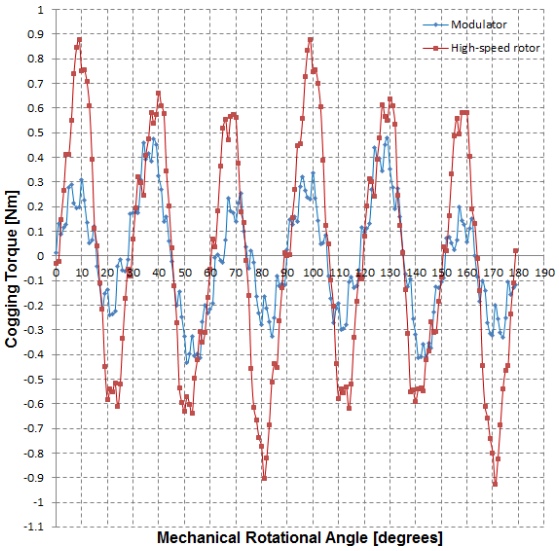

Figure 10: HS rotor and modulator cogging torque.

Fig. 10 further indicates that cogging torque on the high-speed rotor is larger compared to the one experienced by the modulator. This can be expected considering their pole-pairs numbers and respective LCM values.

4.4 Magnetic- and electromagnetic torques

The effect of the gear ratio on both the magnetic- and electromagnetic torques for a 4/6 pole/slot stator combination is shown in Fig. 11. As expected, the electromagnetic torque drops down while the magnetic torque rises as the gear ratio increases. The change in electromagnetic torque can be attributed to the reduction of the coil space area, which implies a reduction of electrical loading.

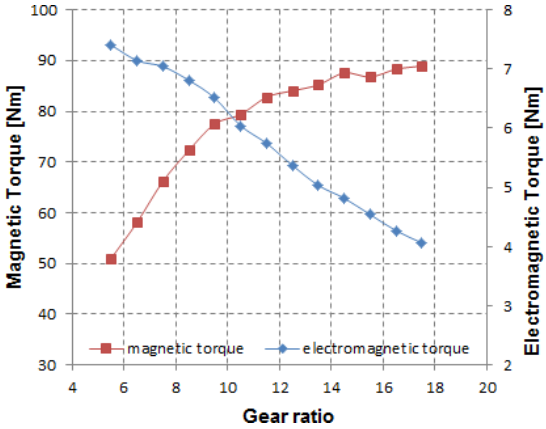

Figure 11: Electromagnetic and magnetic torques vs gear ratios.

Moreover, the change in coil space area is demonstrated by the decrease in stator radial length ($l_{st}+t_{sy}+t_{sb}$) shown in Fig. 12. The implication here is that as the gear ratio increases, the MG uses more space than the PM machine, which could compromise the balance between the two causing the under-design of a stator.

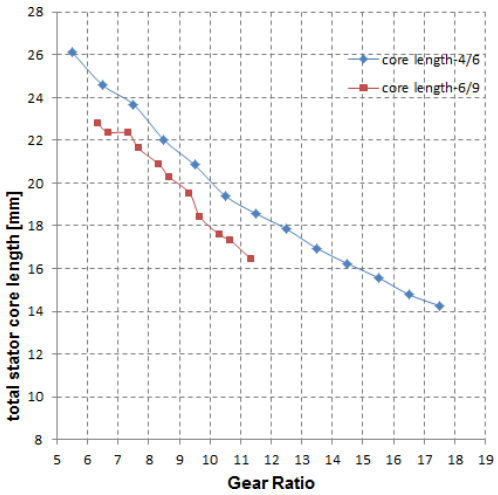

Figure 12: Stator radial length vs gear ratio

5. CONCLUSIONS

In this paper, the structural configuration of the outer-stator magnetically geared PM machine and its basic working principles, especially the torque transmission, have been explained. A dedicated design optimization platform for MGMs was then described. The optimization objective function was solved subject to the demagnetization and stator load factor constraints.

To determine the optimum gear ratio for the MGM with fixed diameter and stack length, the optimization analysis based on 2D static FE solver ran over a range of pole-pair combinations. Meanwhile each set of 2D FE optimized results were further verified in 3D FE analysis for comparison purposes, 2D FE transient simulation was also performed to analyze the core losses of the machine.

The presented simulation results show that the maximum torque of the MGM does reach an optimum value with an increase in the gear ratio. However, the rapid increase of frequency dependent losses with G_r could adversely affect the efficiency of the machine. Careful selection of the stator pole/slot combination could also assist in cogging torque minimization. In addition, the stator capacity is found to decline at larger number of pole-pair combinations.

ACKNOWLEDGMENT

This work was supported in part by ABB AB Corporate Research, Sweden and Stellenbosch University, South Africa

REFERENCES

[1] H. Polinder, F. Van der Pijl, G.-J. de Vilder, and P. Tavner, "Comparison of direct-drive and geared generator concepts for wind turbines," in *Electric Machines and Drives, 2005 IEEE International Conference on*, 2005, pp. 543–550.

[2] P. Rasmussen, T. O. Andersen, F. T. Joergensen, and O. Nielsen, "Development of a high performance magnetic gear," in *Industry Applications Conference, 2003. 38th IAS Annual Meeting. Conference Record of the*, vol. 3, 2003, pp. 1696–1702 vol.3.

[3] K. Atallah, S. Calverley, and D. Howe, "Design, analysis and realisation of a high-performance magnetic gear," *Electric Power Applications, IEE Proceedings* -, vol. 151, no. 2, pp. 135–143, 2004.

[4] K. Atallah, J. Rens, S. Mezani, and D. Howe, "A novel pseudo direct-drive brushless permanent magnet machine," *Magnetics, IEEE Transactions on*, vol. 44, no. 11, pp. 4349–4352, 2008.

[5] D. J. Evans and Z. Zhu, "Influence of design parameters on magnetic gear's torque capability,"

in *Electric Machines Drives Conference (IEMDC), 2011 IEEE International*, 2011, pp. 1403–1408.

[6] T. Lubin, S. Mezani, and A. Rezzoug, "Simple analytical expressions for the force and torque of axial magnetic couplings," *Energy Conversion, IEEE Transactions on*, vol. 27, no. 2, pp. 536–546, 2012.

[7] N. Frank and H. Toliyat, "Gearing ratios of a magnetic gear for wind turbines," in *Electric Machines and Drives Conference, 2009. IEMDC '09. IEEE International*, 2009, pp. 1224–1230.

[8] K. Atallah and D. Howe, "A novel high-performance magnetic gear," *Magnetics, IEEE Transactions on*, vol. 37, no. 4, pp. 2844–2846, 2001.

[9] D. J. Evans and Z. Zhu, "Optimal torque matching of a magnetic gear within a permanent magnet machine," in *Electric Machines Drives Conference (IEMDC), 2011 IEEE International*, 2011, pp. 995–1000.

[10] K. Chau, D. Zhang, J. Jiang, C. Liu, and Y. Zhang, "Design of a magnetic-geared outer-rotor permanent-magnet brushless motor for electric vehicles," *Magnetics, IEEE Transactions on*, vol. 43, no. 6, pp. 2504–2506, 2007.

[11] S. Gerber and R.-J. Wang, "Torque capability comparison of two magnetically geared PM machine topologies," in *Industrial Technology (ICIT), 2013 IEEE International Conference on*, 2013, pp. 1915–1920.

[12] L. Yong, X. Jingwei, P. Kerong, and L. Yongping, "Principle and simulation analysis of a novel structure magnetic gear," in *Electrical Machines and Systems, 2008. ICEMS 2008. International Conference on*, 2008, pp. 3845–3849.

[13] S. E. Skaar, Ø. Krøvel, and R. Nilssen, "Distribution, coil-span and winding factors for PM machines with concentrated windings," in *Electrical Machines (ICEM), 2006 XVII International Conference on*, September 2006.

[14] S. Gerber and R.-J. Wang, "Design of a magnetically geared PM machine," in *Power Engineering, Energy and Electrical Drives (POWERENG), 2013 Fourth International Conference on*, 2013, pp. 852–857.

[15] F. Deng, "An improved iron loss estimation for permanent magnet brushless machines," in *Electric Machines and Drives Conference Record, 1997. IEEE International*, 1997, pp. WB2/3.1–WB2/3.3.

[16] L. Dosiek and P. Pillay, "Cogging torque reduction in permanent magnet machines," *Industry Applications, IEEE Transactions on*, vol. 43, no. 6, pp. 1565–1571, 2007.